基于扩张状态观测器的车辆横摆稳定模型预测控制器设计

曲 逸[1,2], 许 芳[2†], 于树友[2], 陈 虹[3,2], 李宗俐[4]

(1. 吉林大学 汽车与仿真国家重点实验室, 吉林 长春 130025; 2. 吉林大学 通信工程学院, 吉林 长春 130025;
3. 同济大学 新能源汽车工程中心, 上海 201804; 4. 中国一汽集团公司研究设计中心, 山东 青岛 266000)

摘要: 针对车辆横摆稳定性控制问题, 本文提出一种基于扩张状态观测器的线性模型预测控制器设计方法. 首先, 将非线性车辆模型线性化, 建立带有模型误差干扰项的线性模型, 其中线性化导致的模型误差采用扩张状态观测器估计得到, 并证明了观测器的稳定性. 然后基于此模型设计线性预测控制器, 近似实现了非线性预测控制器的控制效果, 同时降低了计算量. 最后, 通过不同路况下的仿真实验结果, 验证了所提方法的计算性能和控制效果.

关键词: 车辆横摆稳定; 模型预测控制; 扩张状态观测器; 不确定扰动

引用格式: 曲逸, 许芳, 于树友, 等. 基于扩张状态观测器的车辆横摆稳定模型预测控制器设计. 控制理论与应用, 2020, 37(5): 941 – 949

DOI: 10.7641/CTA.2019.19018

Model predictive control based on extended state observer for vehicle yaw stability

QU Yi[1,2], XU Fang[2†], YU Shu-you[2], CHEN Hong[3,2], LI Zong-li[4]

(1. State Key Laboratory of Automotive Simulation and Control, Jilin University, Changchun Jilin 130025, China;
2. College of Communication Engineering, Jilin University, Changchun Jilin 130025, China;
3. Clean Energy Automotive Engineering Center, Tongji University, Shanghai 201804, China;
4. China FAW Research and Design Center, Qingdao Shandong 266000, China)

Abstract: In this paper, a linear model predictive control (LMPC) based on extended state observer (ESO) strategy is proposed to improve vehicle stability. Firstly, a linear model with disturbance term is obtained by linearizing the nonlinear vehicle system. The plant-model mismatch and external disturbance are captured by ESO, and its stability is assessed. In the following, estimated disturbance is compensated in the LMPC controller to meet the performance by nonlinear model predictive control (NMPC), and the computational burden is decreased at the same time. Finally, the simulation results under different road conditions verify the computational performance and control effect of the proposed method.

Key words: vehicle yaw stability; model predictive control; extended state observer; uncertain disturbance

Citation: QU Yi, XU Fang, YU Shuyou, et al. Model predictive control based on extended state observer for vehicle yaw stability. *Control Theory & Applications*, 2020, 37(5): 941 – 949

1 Introduction

In recent years, vehicle stability control has received significant attention and become a major research area. Under poor driving conditions, such as extremely wet and snowy roads, most drivers may show panic reactions and become unable to coordinate steering, braking and throttle commands in a timely and effective manner, so that the actual running state of the vehicle and the driver's intention are greatly deviated. The deviations may result in vehicle offset and instability, which put passengers at risk. Therefore, it is necessary to design a vehicle stability control system to intervene the vehicle timely and correct its state before the danger occurs[1].

Nowadays, various methods have been studied for vehicle yaw stability control. The classical control method is PID controller for vehicle safety and stability[2]. However, PID is still not suitable for some complicated and extreme maneuvers in vehicle systems. Hence, many modern control methods have been introduced such as fuzzy logic control, triple-step nonlinear method, sliding mode control and robust control. Fuzzy logic control[3] and triple-step nonlinear method[4] can simplify the nonlinear complexity of vehicle system design. However, the fuzzy rules of the control strategy and the map using in triple-step method are most-

Received 23 January 2019; accepted 25 October 2019.
†Corresponding author. E-mail: fangxu@jlu.edu.cn; Tel.: +86 18343089688.
Recommended by Associate Editor: LIN Zong-li.
Supported by the National Natural Science Foundation of China (61703176, 61573165, 61790564, 61520106008).

ly decided by experience, which would be easily ineffective with unexpected maneuvers. Sliding mode control[5] can achieve fast dynamic response, but the undesirable chattering always exists in the practical application. To reduce the disturbance in vehicle systems, robust control[6–7] is presented. Since the design of robust control is generally based on the worst conditions of systems, the control performance can not get optimal for most situations. Nevertheless, in consider of the multiple requirements and constraints existing in the vehicle systems, model predictive control (MPC) has been introduced to these systems as an effective way to cope with such constrained optimal control problem[8]. MPC is a model-based multivariable control method which aims at solving constrained control problems with optimization demands. Lots of successful papers show that MPC as a practical constrained control algorithm has been applied in many fields[9–11]. Due to the nonlinear terms in vehicle stability control system, nonlinear model predictive control (NMPC) has been applied to achieve good control performance[12–13]. However, there are still some problems that limit its application. For NMPC, the real-time capability should be advanced and the complexity of designing should be reduced[14].

For the past few years, some novel control schemes have been proposed to deal with the computational burden in the vehicle stability control systems using NMPC. An explicit NMPC is proposed in [15], in which the optimization problem is solved off-line. In [16–17], a fast NMPC approach is proposed using an approximated control function and derived by means of set membership (SM) techniques. In addition to the improvements in algorithm, a hardware acceleration is applied in [18] using the field programmable gate array (FPGA). However, compared with LMPC, NMPC is still not superior in computational efficiency.

In order to achieve good control performance on the basis of reducing the computational burden, an LMPC controller based on extended state observer (ESO) is proposed for yaw stability control of in-wheel-motored electric vehicle in this paper. An LMPC controller can be obtained by linearizing the two degrees of freedom (2–DOF) nonlinear vehicle model. The resulting disturbance after linearization is estimated by ESO. ESO is the key link toward the active disturbance rejection control (ADRC) proposed by HAN[19–20]. It is tolerant for most uncertainties in a large degree and not a model based approach which needs accurate mathematical model[21–22]. Based on the advantages above, ESO is added to the control in this paper. With the estimated disturbance compensated in the LMPC controller, the control performance is as good as NMPC approximately, and the computational efficiency is improved significantly compared to NMPC. The initial result on the LMPC controller based on ESO has been studied in our early work[23], which is for the simple single input single output system. To solve the vehicle yaw stability control problem, this paper extends it to a complicated multiple input multiple output system. The simulation results demonstrates its feasibility.

The structure of this paper is as follows. A 2–DOF vehicle model for controller design is built in Section 2. In Section 3, an LMPC controller based on ESO is designed in detail, and the stability of ESO is assessed. The simulation results and analyses are given in Section 4. Finally, the short conclusion is drawn in Section 5.

2 Modeling for controller design

In this section, the construction of 2–DOF vehicle model and tyre model are introduced respectively.

2.1 Vehicle model

Considering that the lateral and yaw motion of vehicle are related to stability closely, only these two degrees of freedom are modeled. The longitudinal speed of the vehicle is assumed to be constant. To simplify the vehicle model, the front two wheels are assumed to have same steering angle. Then the left and right wheels of each axles are lumped into a single wheel. Under the situation that drivers can only manipulate the front wheel steering, a control oriented 2–DOF vehicle model is obtained and shown in Fig.1.

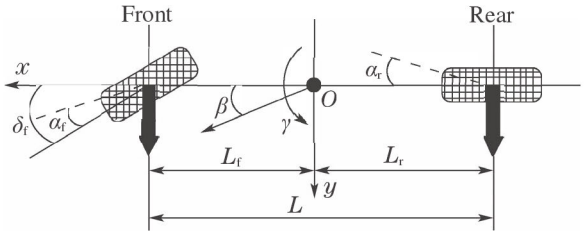

Fig. 1 2–DOF vehicle model

Sideslip angle β and yaw rate γ are selected as state variables. In the vehicle control system, the vehicle lateral motion and torque balance equations are as follows:

$$\begin{cases} \dot{\beta} = \dfrac{F_{\rm yf} + F_{\rm yl}}{mV} - \gamma, \\ \dot{\gamma} = \dfrac{L_{\rm f}F_{\rm yf} - L_{\rm r}F_{\rm yr} + M_{\rm z}}{I_{\rm z}}, \end{cases} \tag{1}$$

where $L_{\rm f}$ and $L_{\rm r}$ are the distance from centroid to the front and rear axle respectively, $I_{\rm z}$ is the moment of inertia, $F_{\rm yf}$ and $F_{\rm yl}$ are the lateral forces of the front and rear wheels of vehicle respectively. The yaw moment of the vehicle $M_{\rm z}$ can be obtained as

$$M_{\rm z} = (-F_{\rm xfl} + F_{\rm xfr} - F_{\rm xrl} + F_{\rm xrr})\frac{w}{2}, \tag{2}$$

where $F_{\rm xfl}$, $F_{\rm xfr}$, $F_{\rm xrl}$, $F_{\rm xrr}$ represent the tyre longitudinal forces, and w is the tread of vehicle.

2.2 Tyre model

Considering that the motion state of vehicle is directly determined by the comprehensive effect of tyre

force, the modeling for tyre characteristics is particularly important. Among the typical tyre models, magic formula tyre model is a relatively mature one for vehicle stability control. It needs only one set of formula to realize the longitudinal and lateral simulation effects of the tyre. The magic formula is as follows:

$$F_{yi} = D\sin(C\arctan(B\alpha_i - E(B\alpha_i - \arctan B\alpha_i))), \tag{3}$$

where α_i is the slip angle of tyre, and C, B, E, D represent the curve shape factor, stiffness factor, longitudinal stiffness and maximum factor respectively. Simplify the formula to suit the controller, then a cubic polynomial is obtained by Taylor expansion as follows:

$$\begin{cases} F_{yf} = -2C_f(1 - K_a\alpha_f^2)\alpha_f, \\ F_{yr} = -2C_r(1 - K_b\alpha_r^2)\alpha_r, \end{cases} \tag{4}$$

K_a and K_b are obtained by tyre magic formula. According to the geometry of vehicle, the tyre sideslip angles of the front and real wheels are as follows:

$$\begin{cases} \alpha_f = \beta + \dfrac{L_f}{V}\gamma - \delta_f, \\ \alpha_r = \beta - \dfrac{L_r}{V}\gamma. \end{cases} \tag{5}$$

In addition, although the pitch and roll motion of vehicle are not included in the vehicle modeling, their effects on the vertical load of the tyre still needs to be considered. Therefore, the vertical load of four wheels in an electric vehicle are calculated. The static loads F_{zf} and F_{zr} can be obtained as follows:

$$F_{zf} = \frac{L_r}{2(L_f + L_r)}mg,\ F_{zr} = \frac{L_f}{2(L_f + L_r)}mg, \tag{6}$$

the dynamic load ΔF_{zfl}, ΔF_{zfr}, ΔF_{zrl}, ΔF_{zrr} are calculated as follows:

$$\begin{cases} \Delta F_{zfl} = -\dfrac{ma_x h}{2(L_f + L_r)} - \dfrac{ma_y h L_r}{w(L_f + L_r)}, \\ \Delta F_{zfr} = -\dfrac{ma_x h}{2(L_f + L_r)} + \dfrac{ma_y h L_r}{w(L_f + L_r)}, \\ \Delta F_{zrl} = \dfrac{ma_x h}{2(L_f + L_r)} - \dfrac{ma_y h L_f}{w(L_f + L_r)}, \\ \Delta F_{zrr} = \dfrac{ma_x h}{2(L_f + L_r)} + \dfrac{ma_y h L_f}{w(L_f + L_r)}, \end{cases} \tag{7}$$

where a_x and a_y are longitudinal and lateral acceleration respectively, h is the height of center of gravity.

3 Control strategy

In this section, we will design an LMPC controller based on ESO in detail. The control requirements and schemes are introduced, and the reference model is presented. In addition, the designed ESO is proved to be stable.

The major reason for the instability of vehicle is that the tyre cannot provide sufficient steering centripetal force when the lateral force is saturated. The yaw rate and sideslip angle of the vehicle are two important variables describing the vehicle posture, which are related to vehicle stability closely. The yaw rate reflects the steady-state turning characteristics, and the sideslip angle reflects the stability of the vehicle. When the sideslip angle is relatively small, the turning speed and turning radius of vehicle are mainly determined by the yaw rate. On the contrary, it will become the main factor which changes the slip angle of tyre. Therefore, in the vehicle yaw stability control system, the main control target is to make the vehicle yaw rate track the desired yaw rate and the sideslip angle as close to zero as possible. A control structure of the vehicle yaw stability system is shown in Fig.2.

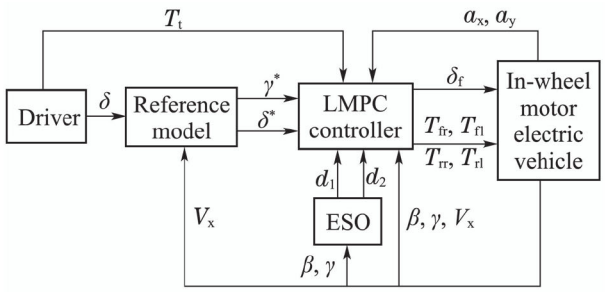

Fig. 2 Control structure of vehicle yaw stability system

As the control structure diagram shows, the driver module is responsible for simulating the driver's driving operation, and providing the steering wheel angle and the driver's desired torque. The vehicle reference model determines the desired yaw rate and sideslip angle according to the steering wheel angle given by driver. Two disturbance signals are generated after linearization, and the disturbance observer is regarded as a multivariable ESO to compensate its real-time estimation to the linear controller. ESO is combined with LMPC controller as the overall controller of the system to provide the front wheel angle and the driving torque of four wheels.

3.1 Reference model

Since this paper studies on the integrated control system of active front steer (AFS) and direct yaw control (DYC), the reference model is described as follows:

$$\begin{cases} \dot{\gamma}^* = -\dfrac{1}{\tau}\gamma^* + \dfrac{k}{\tau}\delta, \\ \beta^* = 0, \end{cases} \tag{8}$$

k and τ are as follows:

$$\begin{cases} k = \dfrac{2C_f V}{mV^2 + 2(C_f L_f - C_r L_r)}, \\ \tau = \dfrac{I_z V}{2(C_f L_f^2 + C_r L_r^2)}, \end{cases} \tag{9}$$

where δ is steering wheel angle, C_f and C_r are the cornering stiffness for front and rear wheel respectively, V represents the vehicle longitudinal speed, m is vehicle mass and I_z represents the moment inertia.

3.2 LMPC controller design

Considering that the yaw rate and sideslip angle are closely related to the vehicle yaw stability, they are chosen as the state variables $x = [\beta\ \ \gamma]^{\mathrm{T}}$. Given that the drive unit contains four in-wheel motors and active steering devices, the front wheel steering angle and motor torque act as control inputs $u = [\delta_{\mathrm{f}}\ \ T_{\mathrm{xfl}}\ \ T_{\mathrm{xfr}}\ \ T_{\mathrm{xrl}}\ \ T_{\mathrm{xrr}}]^{\mathrm{T}}$. Moreover, the state variables are also selected as the output variables $y = [\beta\ \ \gamma]^{\mathrm{T}}$. It is assumed that the output variables β and γ can be obtained by measurement or estimator.

Given that the vehicle yaw stability control system belongs to nonlinear system and the nonlinearity is mainly reflected in the lateral force of tyre as Equation (4) presents, it is necessary to make the linearization for LMPC design. Neglecting the nonlinear terms in Equation (4) directly, the linear expression of lateral force can be obtained as Equation (10). The disturbance term is defined as $d = [d_1\ \ d_2]^{\mathrm{T}}$, which represents the part estimated by ESO after the linearization.

$$\begin{cases} F_{\mathrm{yf}} = -2C_{\mathrm{f}}\alpha_{\mathrm{f}}, \\ F_{\mathrm{yr}} = -2C_{\mathrm{r}}\alpha_{\mathrm{r}}. \end{cases} \tag{10}$$

As the system model introduced in Section 2, the continuous-time model is obtained as follows:

$$\begin{cases} \dot{x}(t) = A_{\mathrm{c}}x(t) + B_{\mathrm{cu}}u(t) + B_{\mathrm{cd}}d(t), \\ y_{\mathrm{c}}(t) = C_{\mathrm{c}}x(t), \end{cases} \tag{11}$$

where

$$\begin{cases} A_{\mathrm{c}} = \begin{bmatrix} -\dfrac{2C_{\mathrm{f}}+2C_{\mathrm{r}}}{mV} & \dfrac{-2C_{\mathrm{f}}L_{\mathrm{f}}+2C_{\mathrm{r}}L_{\mathrm{r}}}{mV^2}-1 \\ \dfrac{-2C_{\mathrm{f}}L_{\mathrm{f}}+2C_{\mathrm{r}}L_{\mathrm{r}}}{I_{\mathrm{z}}} & \dfrac{-2C_{\mathrm{f}}L_{\mathrm{f}}^2-2C_{\mathrm{r}}L_{\mathrm{r}}^2}{I_{\mathrm{z}}V} \end{bmatrix}, \\ B_{\mathrm{cu}} = \begin{bmatrix} \dfrac{2C_{\mathrm{f}}}{mV} & 0 & 0 & 0 & 0 \\ \dfrac{2C_{\mathrm{f}}L_{\mathrm{f}}}{I_{\mathrm{z}}} & \dfrac{w}{2\mathrm{R_e}I_{\mathrm{z}}} & \dfrac{-w}{2\mathrm{R_e}I_{\mathrm{z}}} & \dfrac{w}{2\mathrm{R_e}I_{\mathrm{z}}} & \dfrac{-w}{2\mathrm{R_e}I_{\mathrm{z}}} \end{bmatrix}, \\ B_{\mathrm{cd}} = C_{\mathrm{c}} = \begin{bmatrix} 1 & 0 \\ 0 & 1 \end{bmatrix}. \end{cases} \tag{12}$$

To reduce static error, the continuous-time model is converted into incremental model during the process of discretization by Euler method:

$$\begin{cases} \Delta x(k+1) = A\Delta x(k) + B_{\mathrm{u}}\Delta u(k) + B_{\mathrm{d}}\Delta d(k), \\ y(k) = C\Delta x(k) + y(k-1), \end{cases} \tag{13}$$

where

$$\begin{cases} \Delta x(k) = x(k) - x(k-1), \\ \Delta u(k) = u(k) - u(k-1), \\ \Delta d(k) = d(k) - d(k-1). \end{cases} \tag{14}$$

According to the MPC's principle, m is defined as control horizon and p is defined as predictive horizon, $m \leqslant p$. In this paper, vehicle velocity and disturbances estimated by ESO are supposed to be constant in predictive horizon. Based on the model described in Equation (13), incremental sequence of control input in p step at time k is obtained as follows. It is chosen as an independent variable for constrained optimization problems:

$$\Delta U(k) = \begin{bmatrix} \Delta u(k) \\ \Delta u(k+1) \\ \vdots \\ \Delta u(k+m-1) \end{bmatrix}_{m\times 1}, \tag{15}$$

the predicted control output sequence is written as

$$Y_p(k+1|k) = \begin{bmatrix} y(k+1|k) \\ y(k+2|k) \\ \vdots \\ y(k+p|k) \end{bmatrix}_{p\times 1}, \tag{16}$$

it can be calculated as

$$\begin{aligned} Y_p(k+1|k) = {} & S_{\mathrm{x}}\Delta x(k) + \tau y(k) + S_{\mathrm{d}}d(k) + \\ & S_{\mathrm{u}}\Delta U(k) \end{aligned} \tag{17}$$

where S_{x}, S_{d} and S_{u} can be derived from the coefficients of Equation (13).

Moreover, according to the reference model introduced in Section 2, the control output reference sequence is obtained as

$$R(k+1|k) = \begin{bmatrix} r(k+1|k) \\ r(k+2|k) \\ \vdots \\ r(k+p|k) \end{bmatrix}_{p\times 1}. \tag{18}$$

In consideration of control requirements, the output Y_p is supposed to track the reference sequence R closely to achieve vehicle yaw stability. Therefore, the deviation between them should be minimized as much as possible, and the first cost function is obtained as

$$\begin{aligned} J_1 = {} & \sum_{i=1}^{p} [(\beta(k+i|k) - \beta^*(k))^2\Gamma_{\mathrm{y1}} + \\ & (\gamma(k+i|k) - \gamma^*(k))^2\Gamma_{\mathrm{y2}}] = \\ & \|\Gamma_{\mathrm{y}}(Y_{p,c}(k+1|k) - R(k+1))\|^2. \end{aligned} \tag{19}$$

From another perspective, the second cost function is obtained to achieve smooth control.

$$\begin{aligned} J_2 = {} & \sum_{i=0}^{m-1} [\Gamma_{u1}(\Delta\delta_{\mathrm{f}}(k+i|i)^2 + \Gamma_{\mathrm{u2}}(\Delta T_{\mathrm{fl}}(k+i|i)^2 + \\ & \Delta T_{\mathrm{fr}}(k+i|i)^2 + \Delta T_{\mathrm{rl}}(k+i|i)^2 + \\ & \Delta T_{\mathrm{rr}}(k+i|i)^2)] = \|\Gamma_{\mathrm{u}}\Delta U(k)\|^2. \end{aligned} \tag{20}$$

Furthermore, in order to minimize the energy consumption and the longitudinal force of tyre under the constraints, the third cost function can be obtained as

$$\begin{aligned} J_3 = {} & \sum_{i=0}^{m-1} [\Gamma_{\mathrm{t}}((\frac{T_{\mathrm{fl}}(k+i|i)}{\mu\mathrm{R_e}F_{\mathrm{zfl}}})^2 + (\frac{T_{\mathrm{fr}}(k+i|i)}{\mu\mathrm{R_e}F_{\mathrm{zfr}}})^2 + \\ & (\frac{T_{\mathrm{rl}}(k+i|i)}{\mu\mathrm{R_e}F_{\mathrm{zrl}}})^2 + (\frac{T_{\mathrm{rr}}(k+i|i)}{\mu\mathrm{R_e}F_{\mathrm{zrr}}})^2)] = \end{aligned}$$

$$\|\Gamma_{\mathrm{T}} A_{\mathrm{J}}(U(k-1) + I_m \Delta U(k))\|^2, \tag{21}$$

where μ, $\mathrm{R_e}$ and F_{zj} are the friction coefficient, wheel radius and vertical load of the four wheels introduced in Section 2, and F_{zj} are constant in the predictive horizon. Through the derivation, A_{J}, I_m and Γ_{T} can be obtained as follows:

$$A_{\mathrm{J}} = \mathrm{diag}\{a_{\mathrm{j}}, \cdots, a_{\mathrm{j}}\}_{4m\times 5m}, \tag{22}$$

where

$$a_{\mathrm{j}} = \begin{bmatrix} 0 & 1 & 0 & 0 & 0 \\ 0 & 0 & 1 & 0 & 0 \\ 0 & 0 & 0 & 1 & 0 \\ 0 & 0 & 0 & 0 & 1 \end{bmatrix}, \tag{23}$$

I_m is defined as

$$I_m = \begin{bmatrix} I_{5\times 5} & & & \\ I_{5\times 5} & I_{5\times 5} & & \\ \cdots & \cdots & & \\ I_{5\times 5} & I_{5\times 5} & \cdots & I_{5\times 5} \end{bmatrix}_{5m\times 5m} \tag{24}$$

as for Γ_{T}, define $\Gamma_{\mathrm{T}i} = (\Gamma_{ti} \times \dfrac{1}{\mu \mathrm{R_e} F_{zi}})_{m\times m}$, then we can obtain that $\Gamma_{\mathrm{T}} = \mathrm{diag}\{\Gamma_{\mathrm{T}1}, \Gamma_{\mathrm{T}2}, \Gamma_{\mathrm{T}3}, \Gamma_{\mathrm{T}4}\}$.

Considering that MPC can deal with multi-objective optimization control problem, the three parts mentioned above can be integrated as

$$\begin{aligned} J = {} & \|\Gamma_{\mathrm{y}}(Y_{p,c}(k+1|k) - R(k+1))\|^2 + \\ & \|\Gamma_{\mathrm{u}} \Delta U(k)\|^2 + \\ & \|\Gamma_{\mathrm{T}} A_{\mathrm{J}}(U(k-1) + I_m \Delta U(k))\|^2, \end{aligned} \tag{25}$$

where Γ_{y}, Γ_{u} and Γ_{T} are weighting matrixes that can be used to adjust the control performance. Ignore the items which not related to $\Delta U(k)$, the equivalent form of the optimization is obtained as

$$\widetilde{J} = \Delta^{\mathrm{T}} U(k) H \Delta U(k) - G(k+1|k)^{\mathrm{T}} \Delta U(k), \tag{26}$$

where

$$\begin{cases} G(k+1|k) = -2I_m^{\mathrm{T}} A^{\mathrm{T}} \Gamma_{\mathrm{T}}^{\mathrm{T}} \Gamma_{\mathrm{T}} A U(k-1) + \\ \qquad\qquad 2S_{\mathrm{u}}^{\mathrm{T}} \Gamma_{\mathrm{y}}^{\mathrm{T}} \Gamma_{\mathrm{y}} E_p(k+1|k), \\ E_p(k+1|k) = R(k+1) - S_{\mathrm{x}} \Delta x(k) - \\ \qquad\qquad \mathcal{I} y_{\mathrm{c}}(k) - S_{\mathrm{d}} \Delta d(k), \\ H = I_m^{\mathrm{T}} A^{\mathrm{T}} \Gamma_{\mathrm{T}}^{\mathrm{T}} \Gamma_{\mathrm{T}} A I_m + \Gamma_{\mathrm{u}}^{\mathrm{T}} \Gamma_{\mathrm{u}} + \\ \qquad S_{\mathrm{u}}^{\mathrm{T}} \Gamma_{\mathrm{y}}^{\mathrm{T}} \Gamma_{\mathrm{y}} S_{\mathrm{u}}. \end{cases} \tag{27}$$

In addition, aiming at achieving desired control performance, the constraints should be considered in the design of MPC. Due to motor torque saturation, the system had better satisfy the following constraint:

$$T_{\min} \leqslant T_i \leqslant T_{\max},\ i = fl, fr, rl, rr. \tag{28}$$

Simultaneously, the sum of torques for each motor are supposed to be equal to the total required one as follows:

$$\sum T_i = T_{\mathrm{t}},\ i = fl, fr, rl, rr. \tag{29}$$

3.3 ESO Design

Owing to the plant-model mismatch caused by model linearization (Equation (10)), ESO is designed to capture the plant-model mismatch and external disturbance. Then the estimated disturbance is compensated in the LMPC controller to obtain a better performance.

For vehicle yaw stability control system in this paper, two disturbance variables d_1 and d_2 in the linear predictive model are supposed to be extended into two new state variables $\omega_1 = d_1$ and $\omega_2 = d_2$ to form the extended system as follows:

$$\begin{aligned} \begin{bmatrix} \dot{\beta} \\ \dot{\gamma} \\ \dot{\omega}_1 \\ \dot{\omega}_2 \end{bmatrix} = {} & \begin{bmatrix} A_{\mathrm{c}2\times 2} & I_{2\times 2} \\ O_{2\times 2} & O_{2\times 2} \end{bmatrix} \begin{bmatrix} \beta \\ \gamma \\ \omega_1 \\ \omega_2 \end{bmatrix} + \\ & \begin{bmatrix} B_{\mathrm{cu}2\times 5} \\ O_{2\times 5} \end{bmatrix} \begin{bmatrix} \delta_{\mathrm{f}} \\ T_{\mathrm{fr}} \\ T_{\mathrm{fl}} \\ T_{\mathrm{rr}} \\ T_{\mathrm{rl}} \end{bmatrix} + \begin{bmatrix} 0 \\ 0 \\ p_1 \\ p_2 \end{bmatrix}, \end{aligned} \tag{30}$$

where A_{c}, B_{cu} are obtained by incremental model as Equation (11). In order to ensure the convergence of the observer, assume that $\dot{\omega}_1 = p_1$ and $\dot{\omega}_2 = p_2$ are both bounded by constant. For the extended linear predictive model, the following form of multi-variable ESO is designed.

$$\begin{bmatrix} \dot{z}_1 \\ \dot{z}_2 \\ \dot{z}_3 \\ \dot{z}_4 \end{bmatrix} = A_{\mathrm{z}} \begin{bmatrix} z_1 \\ z_2 \\ z_3 \\ z_4 \end{bmatrix} + B_{\mathrm{z}} \begin{bmatrix} \delta_{\mathrm{f}} \\ T_{\mathrm{fr}} \\ T_{\mathrm{fl}} \\ T_{\mathrm{rr}} \\ T_{\mathrm{rl}} \end{bmatrix} + C_{\mathrm{z}} \begin{bmatrix} e_1 \\ e_2 \end{bmatrix}, \tag{31}$$

where

$$\begin{cases} A_{\mathrm{z}} = \begin{bmatrix} A_{\mathrm{c}2\times 2} & I_{2\times 2} \\ O_{2\times 2} & O_{2\times 2} \end{bmatrix},\ C_{\mathrm{z}} = \begin{bmatrix} -L_{01} & 0 \\ 0 & -L_{02} \\ -L_{11} & 0 \\ 0 & -L_{12} \end{bmatrix}, \\ B_{\mathrm{z}} = \begin{bmatrix} B_{\mathrm{cu}2\times 5} \\ O_{2\times 5} \end{bmatrix}. \end{cases} \tag{32}$$

For the multi-variable ESO designed above, we can obtain that z_1, z_2, z_3 and z_4 are dynamic estimations of β, γ, d_1 and d_2 respectively. Define the dynamics of the estimate error as

$$\begin{cases} \begin{bmatrix} \dot{e}_1 \\ \dot{e}_2 \\ \dot{e}_3 \\ \dot{e}_4 \end{bmatrix} = \begin{bmatrix} \dot{z}_1 - \dot{\beta} \\ \dot{z}_2 - \dot{\gamma} \\ \dot{z}_3 - \dot{\omega}_1 \\ \dot{z}_4 - \dot{\omega}_2 \end{bmatrix} = A_{\mathrm{e}} \begin{bmatrix} e_1 \\ e_2 \\ e_3 \\ e_4 \end{bmatrix} + \begin{bmatrix} 0 \\ 0 \\ p_1 \\ p_2 \end{bmatrix}, \\ A_{\mathrm{e}} = \begin{bmatrix} A_{\mathrm{c}} - L_{e0} & I_{2\times 2} \\ -L_{e1} & O_{2\times 2} \end{bmatrix}, \end{cases} \tag{33}$$

where $L_{e0} = \mathrm{diag}\{L_{01}, L_{02}\}$, $L_{e1} = \mathrm{diag}\{L_{11}, L_{12}\}$. As long as A_{e} is chosen to be Hurwitz matrix, the dy-

namics of the estimate error is input-to-state stable for p_1 and p_2.

Remark 1 The related works of disturbance observer based MPC was reported in [24–27], which utilizes numerical solutions in the optimization problem. The offset-free MPC by augmenting the system with disturbance model was studied in [24] and [25] for linear systems, in [26] for nonlinear systems, and in [27] for reference tracking problems. These works took the disturbance estimation and its prediction into account in the receding optimization process and achieved zero offset. The recursive feasibility of the optimization problem was guaranteed by tightening the terminal region and the input constraint was studied in[28] for tracking the wheeled mobile robot. Based on aforementioned methods, the stability analysis of the combination of LMPC and ESO will be our future work of the paper.

4 Simulation

In this section, the simulation results in Simulink/MATLAB are presented to verify the method proposed in this paper. A seven degrees of freedom (7–DOF) vehicle model including the yaw of longitudinal, lateral and vertical of the vehicle and the rotation of 4 wheels is built on the simulation platform as follows in Fig.3. The specific model parameters are shown in Table 1.

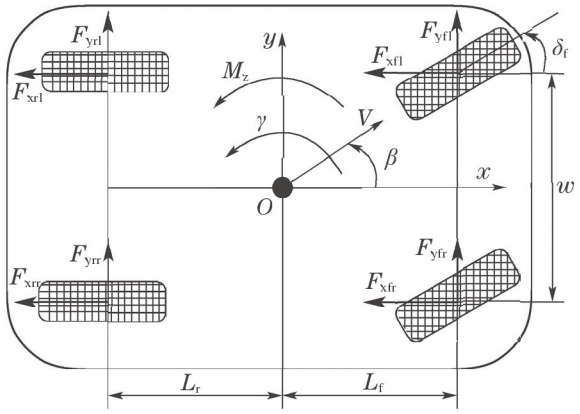

Fig. 3 7–DOF vehicle model

Table 1 Model parameters

Parameter	Value	Unit
vehicle mass m	1359.8	kg
vehicle yaw moment of inertia I_z	1992.54	kg·m^2
tread of vehicle w	1.418	m
centroid to front axle distance L_f	1.0628	m
centroid to rear axle distance L_r	1.4852	m
cornering stiffness at front tire C_f	23540	N/rad
cornering stiffness at rear tire C_r	23101	N/rad
wheel radius R_e	0.29	m
motor maximum torque T_{max}	187	Nm

The reference steering wheel input curve is given in Fig. 4. Set the sampling time to 10 ms. The predictive horizon p and control horizon m are equal to 10 and 3 respectively. As for the observer parameter, they are set as $L_{01} = 20$, $L_{02} = 40$, $L_{11} = 100$, $L_{12} = 200$, then it satisfies the condition that A_e is Hurwitz matrix.

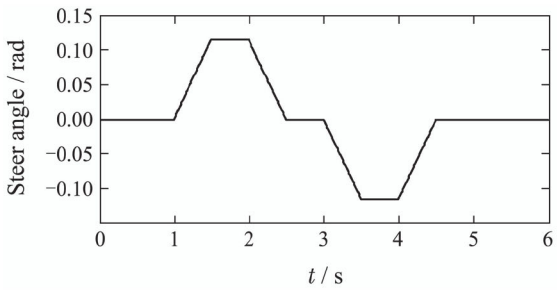

Fig. 4 Steer input curve

For different driving maneuvers, the effectiveness of the controller is analyzed. In the first maneuver, the initial speed is 80 km/h, and friction coefficient is set to 0.8. The designed LMPC controller based on ESO is applied to the vehicle yaw stability control system as shown in Fig.5. In addition, the result of an NMPC controller is presented for comparison in Fig.6.

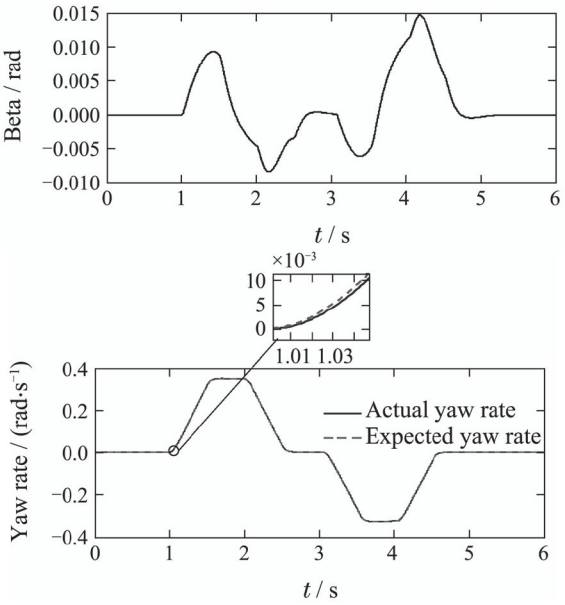

Fig. 5 Simulation results of LMPC based on ESO when $\mu = 0.8$

In each figure, dashed line represents the expected output of system, and the solid one represents the actual output. The comparison shows that the performance of the two controllers are basically the same. On the basis of analysis, it is shown that the tyre lateral force is in the linear area consistently in this maneuver.

To excite the nonlinearity of the lateral tyre force, the friction coefficient is changed to 0.4 as the second maneuver. Then the simulation results form two controllers are presented in Figs.7–8.

Comparing the control performance of LMPC controller based on ESO with NMPC controller, it can be

obtained that they are basically the same although in such nonlinear situation. Furthermore, in order to compare the tracking performance more obviously, the error curves between expected yaw rate and the actual one are presented in Fig.9.

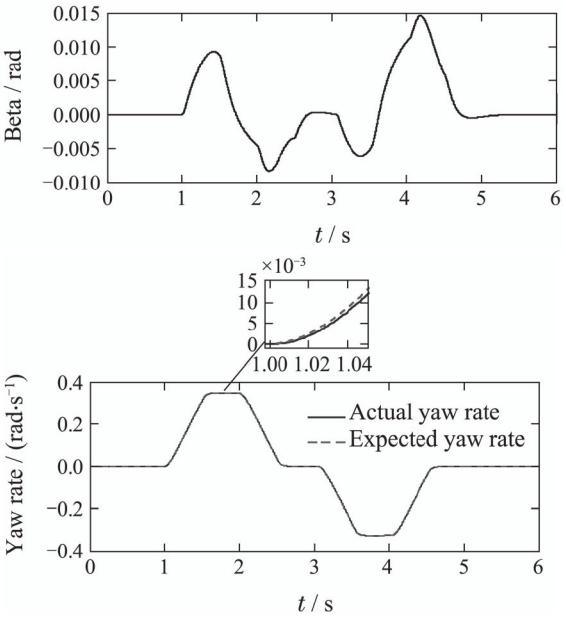

Fig. 6 Simulation results of NMPC when $\mu = 0.8$

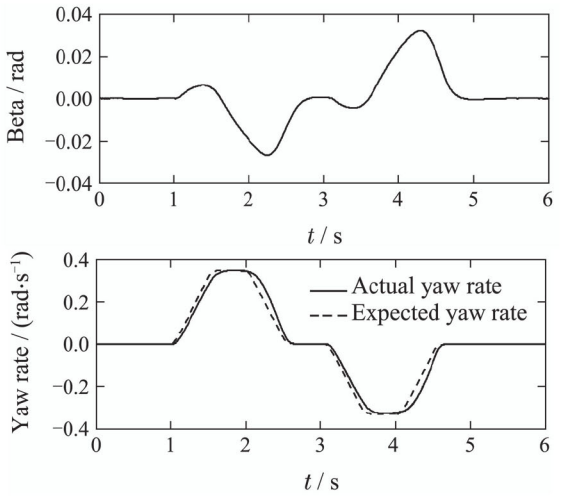

Fig. 7 Simulation results of LMPC based on ESO when $\mu = 0.4$

From the error curves, it proves that the proposed LMPC based on ESO control strategy has the ability to improve the control performance compared to LMPC. What is even more exciting is that this strategy can achieve as good control performance as NMPC. In addition, to make the comparison more intuitively, the standard deviation of each controller is calculated as follows:

$$\sigma = \sqrt{\frac{1}{N}\sum_{i=1}^{N}(e_i - \bar{e})^2}, \tag{34}$$

where $e_i = \gamma_i{}^* - \gamma_i$.

After the calculation, the standard deviations from these three controllers are obtained successively. The results of LMPC, NMPC and LMPC based on ESO are 0.0287, 0.0237 and 0.0238 in turn.

In the case of first maneuver, the lateral tyre force is always in linear area, so that the predictive model is basically a linear model. Nevertheless, in the case of second maneuver, the friction coefficient is reduced, and it leads the vehicle to a limit maneuver during the operation, then the lateral tyre force gets the nonlinear term occurred as a result. In this situation, single LMPC can not track the desired yaw rate well and make the sideslip angle close to zero. By contrast, the LMPC controller based on ESO proposed in this paper can basically achieve the control performance consistent with NMPC controller. Owing to the fact that the plant-model mismatch and external disturbance can be captured and compensated in the LMPC controller, the control performance is improved by using a disturbance feedforward control. However, this strategy proposed in this paper is only applicable to the weakly nonlinear systems with slow changing disturbances.

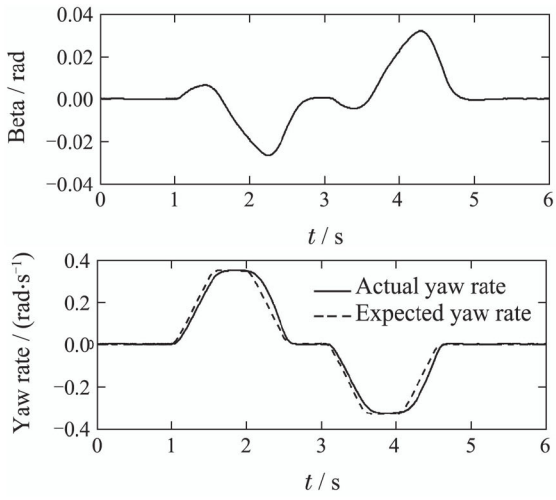

Fig. 8 Simulation results of NMPC when $\mu = 0.4$

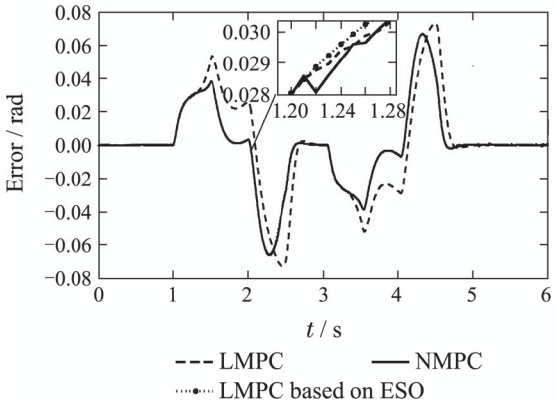

Fig. 9 Tracking error with friction coefficient 0.4 by LMPC, NMPC and LMPC based on ESO

In order to verify the advantages of the method proposed in this paper in computational performance, the comparison results of the solution time on MATLAB platform of LMPC based on ESO and NMPC are presented as shown in Fig.10. The simulation platform is configured as 64–bit Windows 7 PC (CPU Intel Core i7–4790@3.60 GHz, 8 GB memory), MATLAB2014a.

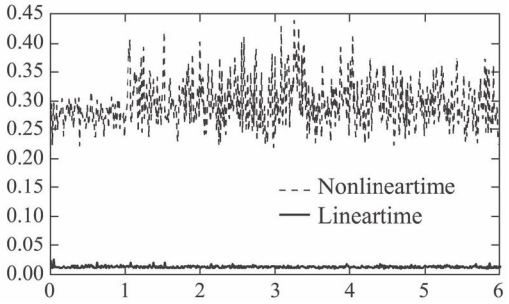

Fig. 10 The comparison results of solution time

The results show that the time of solving one optimization problem using NMPC is about 0.35 s, while it is about 0.025 s using LMPC based on ESO. It can be seen that computational time can be greatly reduced on the premise of ensuring consistent control performance.

5 Conclusion

A novel method of LMPC controller based on ESO is proposed for vehicle yaw stability control system in this paper, which can reduce the computational burden to some extent compared to NMPC controller in practical application. ESO is used to estimate the disturbance to compensate modeling error caused by linearization, and its stability is proved simultaneously. The simulation results demonstrate that the nonlinear term would appear when the vehicle is approaching extreme conditions. At this time, ESO-based LMPC can meet the control requirements as NMPC. The sideslip angle is close to zero, and the yaw rate can track its reference value well, which satisfy the control requirements effectively.

References:

[1] WANG J M, LONGORIA R G. Coordinated and reconfigurable vehicle dynamics control. *IEEE Transactions on Control Systems Technology*, 2009, 17(3): 723 – 732.

[2] SHI Y, YU F. Hierarchical direct yaw-moment control system design for in-wheel motor driven electric vehicle. *International Journal of Automotive Technology*, 2018, 19(4): 695 – 703.

[3] KRISHNA S, NARAYANAN S, ASHOK S D. Fuzzy logic based yaw stability control for active front steering of a vehicle. *Journal of Mechanical Science and Technology*, 2014, 28(12): 5169 – 5174.

[4] ZHAO H Y, GAO B Z, REN B T, et al. Integrated control of in-wheel motor electric vehicles using a triple-step nonlinear method. *Journal of the Franklin Institute*, 2015, 352(2): 519 – 540.

[5] BAGHERI A, AZADI S, SOLTANI A. A combined use of adaptive sliding mode control and unscented kalman filter estimator to improve vehicle yaw stability. *Proceedings of the Institution of Mechanical Engineers, Part K: Journal of Multi-body Dynamics*, 2017, 231(2): 388 – 401.

[6] JIN X J, YIN G D, ZENG X H, et al. Robust gain-scheduled output feedback yaw stability control for in-wheel-motor-driven electric vehicles with external yaw-moment. *Journal of the Franklin Institute*, 2018, 355(18): 9271 – 9297.

[7] HU J S, WANG Y F, FUJIMOTO H, et al. Robust yaw stability control for in-wheel motor electric vehicles. *IEEE/ASME Transactions on Mechatronics*, 2017, 22(3): 1360 – 1370.

[8] YU K J, YANG J Q, YAMAGUCHI D. Model predictive control for hybrid vehicle ecological driving using traffic signal and road slope information. *Control Theory and Technology*, 2015, 13(1): 17 – 28.

[9] GUO L L, GAO B Z, LI Y, et al. A fast algorithm for nonlinear model predictive control applied to hev energy management systems. *Science China Information Sciences*, 2017, 60(9): 092201.

[10] BONNE F, ALAMIR M, BONNAY P. Experimental investigation of control updating period monitoring in industrial plc-based fast MPC: Application to the constrained control of a cryogenic refrigerator. *Control Theory and Technology*, 2017, 15(2): 92 – 108.

[11] NAIR R R, BEHERA L. Robust adaptive gain higher order sliding mode observer based control-constrained nonlinear model predictive control for spacecraft formation flying. *IEEE/CAA Journal of Automatica Sinica*, 2018, 5(1): 367 – 381.

[12] REN B T, CHEN H, ZHAO H Y, et al. Mpc-based yaw stability control in in-wheel-motored ev via active front steering and motor torque distribution. *Mechatronics*, 2016, 38: 103 – 114.

[13] LI S S, WANG G D, GUO L P, et al. NMPC-based yaw stability control by active front wheel steering. *IFAC–PapersOnLine*, 2018, 51(31): 583 – 588.

[14] XI Y G, LI D W, LIN S. Model predictive control-status and challenges. *Acta Automatica Sinica*, 2013, 39(3): 222 – 236.

[15] METZLER M, TAVERNINI D, SORNIOTTI A, et al. An explicit nonlinear mpc approach to vehicle stability control. *Proceedings of The 14th International Symposium on Advanced Vehicle Control*. Beijing: Tsinghua University, 2018.

[16] CANALE M, FAGIANO L, RAZZA V. Approximate nmpc for vehicle stability: design, implementation and sil testing. *Control Engineering Practice*, 2010, 18(6): 630 – 639.

[17] CANALE M, FAGIANO L. Vehicle yaw control using a fast nmpc approach. *The 47th IEEE Conference on Decision and Control*. Cancun, Mexico: IEEE 2008: 5360 – 5365.

[18] GUO H Y, LIU F, XU F, et al. Nonlinear model predictive lateral stability control of active chassis for intelligent vehicles and its FPGA implementation. *IEEE Transactions on Systems, Man, and Cybernetics: Systems*, 2019, 49(1): 2 – 13.

[19] HAN J Q. *Active Disturbance Rejection Control Technique-the Technique for Estimating and Compensating the Uncertainties*. Beijing: National Defense Industry Press, 2008: 197 – 270.

[20] HAN J Q. From pid to active disturbance rejection control. *IEEE Transactions on Industrial Electronics*, 2009, 56(3): 900 – 906.

[21] XIONG S F, WANG W H, LIU X D, et al. A novel extended state observer. *ISA Transactions*, 2015, 58: 309 – 317.

[22] ZHENG Q, GAO Z Q. Active disturbance rejection control: some recent experimental and industrial case studies. *Control Theory and Technology*, 2018, 16(4): 301 – 313.

[23] LI Z L, XU F, LIANG D N, et al. Design of model predictive controller based on extended state observer. *Control and Decision Conference (CCDC)*. Chongqing, China: IEEE, 2017: 7421 – 7426.

[24] PANNOCCHIA G, BEMPORAD A. Combined design of disturbance model and observer for offset-free model predictive control. *IEEE Transactions on Automatic Control*, 2007, 52(6): 1048 – 1053.

[25] MAEDER U, BORRELLI F, MORARI M. Linear offset-free model predictive control. *Automatica*, 2009, 45(10): 2214 – 2222.

[26] MORARI M, MAEDER U. Nonlinear offset-free model predictive control. *Automatica*, 2012, 48(9): 2059 – 2067.

[27] MAEDER U, MORARI M. Offset-free reference tracking with model predictive control. *Automatica*, 2010, 46(9): 1469 – 1476.

[28] SUN Z Q, XIA Y Q, DAI L, et al. Disturbance rejection MPC for tracking of wheeled mobile robot. *IEEE/ASME Transactions on Mechatronics*, 2017, 22(6): 2576 – 2587.

作者简介:

曲 逸 硕士研究生, 目前研究方向为预测控制的算法研究及FPGA技术在汽车控制系统中的应用, E-mail: quyeeee@163.com.cn;

许 芳 副教授, 目前研究方向为预测控制的算法研究及FPGA技术在汽车控制中的应用, E-mail: fangxu@jlu.edu.cn;

于树友 教授, 目前研究方向为模型预测控制及其在汽车控制中的应用, E-mail: yushuyou@126.com;

陈 虹 教授, 目前研究方向为模型预测控制、鲁棒控制、非线性控制以及其在汽车控制系统中的应用, E-mail: chenh@jlu.edu.cn;

李宗俐 工程师, 目前研究方向为FPGA技术在汽车控制中的应用, E-mail: sdrzlzl@126.com.